An Industrially Viable Catalyst System for Palladium-Catalyzed Telomerizations of 1,3-Butadiene with Alcohols

Ralf Jackstell,[a] Surendra Harkal,[a] Haijun Jiao,[a] Anke Spannenberg,[a] Cornelia Borgmann,[b] Dirk Röttger,[b] Franz Nierlich,[b] Mark Elliot,[c] Stuart Niven,[c] Kingsley Cavell,[c] Oscar Navarro,[d] Mihai S. Viciu,[d] Steven P. Nolan,[d] and Matthias Beller*[a]

Abstract: The telomerization reaction of 1,3-butadiene with alcohols to give alkyl octadienyl ethers in the presence of palladium–carbene catalysts has been studied in detail. Unprecedented catalyst efficiency with turnover numbers (TON) up to 1500000 and turnover frequencies (TOF) up to 100000 h^{-1} have been obtained after optimization for the reaction of methanol in the presence of an excess of in situ generated carbene ligands. High yields (75–97%) and catalyst productivities (TON 15000–100000) are observed for other aliphatic alcohols and phenols. For comparison five carbene–palladium(0) complexes have been synthesized and characterized by X-ray crystallography. Both electronic and steric effects on the stability and reactivity of the catalysts have been discussed on the basis of density functional theory calculations.

Keywords: butadiene · carbene · homogeneous catalysis · palladium · telomerization

Introduction

An important goal in organic chemistry is the development of green processes that use fewer raw materials and less energy, maximize the use of renewable resources, and minimize or eliminate the use of dangerous chemicals. Clearly, none of this is possible without catalysis. In general as the science of accelerating chemical reactions, catalysis is about using value-added transformations to convert simple raw materials to more complex molecules with versatile application characteristics. In this regard the palladium-catalyzed telomerization of 1,3-dienes with nucleophiles is an interesting methodology, that combines simple starting materials in a 100% atom efficient manner to give functionalized octa-2,7-dienes.[1,2] Due to their ready availability and low price,[3] 1,3-butadiene and alcohols, especially methanol, are attractive starting materials for this reaction (Scheme 1).

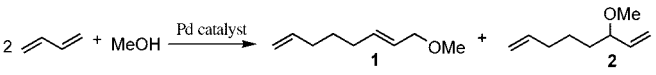

Scheme 1. Telomerization of 1,3-butadiene with methanol.

The reaction usually leads to a mixture of *cis*/*trans* isomers where 1-methoxyocta-2,7-diene **1** (*n*-products) is in general the major product, which is a useful precursor for plasticizer alcohols (octanols), solvents, corrosion inhibitors, and monomers for polymers.[4] In addition, the by-products of this reaction, mainly the 3-substituted methoxyocta-1,7-dienes **2** (*iso*-products), 1,3,7-octatriene and 4-vinylcyclohexene (VCH) also are of some commercial interest. Hence, this telomerization process has been the subject of intensive research in both academic and industrial laboratories.[5]

Important mechanistic studies of the telomerization of methanol and 1,3-butadiene in the presence of palladium/phosphine catalysts have been performed by Jolly and co-

[a] Dr. R. Jackstell, S. Harkal, Dr. H. Jiao, Dr. A. Spannenberg, Prof. Dr. M. Beller
Leibniz-Institut für Organische Katalyse
an der Universität Rostock e.V.
Buchbinderstrasse 5–6
18055 Rostock (Germany)
Fax: (+49) 381-46693-24
E-mail: matthias.beller@ifok.uni-rostock.de

[b] Dr. C. Borgmann, Dr. D. Röttger, Dr. F. Nierlich
Degussa AG, OXENO C4-Chemie
Paul-Baumann-Strasse 1, 45764 Marl (Germany)

[c] Dr. M. Elliot, S. Niven, Prof. Dr. K. Cavell
Cardiff University
PO Box 912, Cardiff CF 10 3TB, Wales (UK)

[d] O. Navarro, M. S. Viciu, Prof. Dr. S. P. Nolan
University of New Orleans
Department of Chemistry
New Orleans, Louisiana 70148 (USA)

 DOI: 10.1002/chem.200400182

workers.[6] More recently, we also investigated this reaction, which led to an extended mechanistic proposal.[7] As shown in Scheme 2, it is proposed that in the presence of palladium(0) species, two molecules of 1,3-butadiene couple to form the [$PdPPh_3(\eta^1,\eta^3$-octadiendiyl)] complex **3**. Protonation of **3** by methanol at the C6 atom of the C_8 chain leads to the [$PdPPh_3(\eta^2,\eta^3$-C_8H_{13})] species **4**.

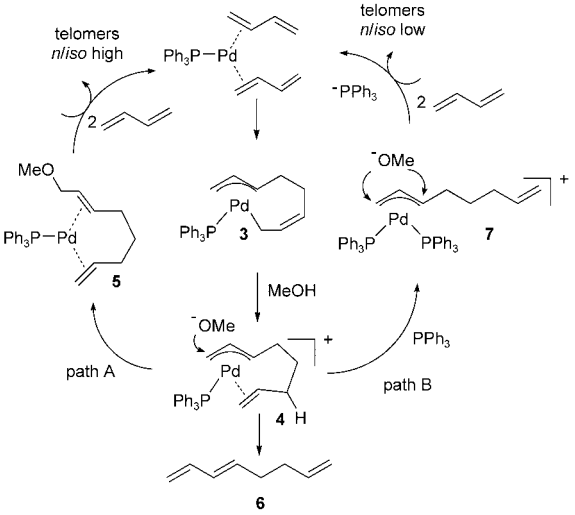

Scheme 2. Proposed mechanism for the telomerization of 1,3-butadiene with methanol.

In the following step of the reaction (path A), the methoxide ion adds to either the allylic terminus C1 or C3 of the C_8 chain resulting in the formation of the telomers **1** or **2**, respectively. The formation of 1,3,7-octatriene **6** can occur as a side reaction by β-hydrogen elimination from C4 in **4**. Clearly, the regioselectivity determining step of the process is the nucleophilic attack of methanol or methoxide ion on the π-allylpalladium(phosphine) complex **4**. The nucleophilic attack at the C1 atom is favored for steric reasons, while the attack at C3 atom is electronically favored.[8] Moreover, the linear telomer is the thermodynamically more stable product due to the presence of an internal double bond, whereas the branched isomer with the terminal double bond is less thermodynamically stable.

The selective formation of the linear telomer 1-methoxy-octa-2,7-diene **1** is influenced to a large extent by the ligand to metal ratio and the stoichiometry of the starting materials. Good *n*/*iso*-selectivities (up to 97%) are realized at low P and Pd ratio (1:1) and high methanol to 1,3-butadiene ratios in the absence of other coordinating species. A second ligand, for example, phosphine bound to the metal center, reduces the regioselectivity dramatically. This explains the formation of **7**, which leads to lower *n*/*iso*-selectivity compared with **4** (reaction path B). Here, the regioselectivity of the nucleophilic attack of methoxide anion on the allyl palladium intermediate is no longer determined by the formation of the favorable complex **5** with a chelating 1,6-diene ligand. Hence, the internal coordination of the olefinic side chain is one of the main driving forces governing the *n*/*iso*-selectivity.

Despite the economic attractiveness of the starting materials, a prerequisite for an industrial use of this telomerization reaction is the required high catalyst efficiency due to the relatively high price of palladium.[9] From the catalytic cycle of the reaction it is apparent that only one external ligand (L) on the palladium center is sufficient for a productive and highly selective catalyst system. Importantly, L should be sterically demanding in order to prevent palladium agglomeration and simple coordination of a second ligand L, which leads to a lower *n*/*iso*-selectivity.

Inspired by the aforementioned catalytic cycle we thought that stable palladium(0)–1,6-diene complexes resembling the catalytic intermediate **5** should be ideal catalyst systems. Unfortunately, the corresponding (phosphine)palladium(0)–1,6-diene[10] complexes did not prove to be superior for telomerizations compared to the standard phosphine/palladium(II) pre-catalysts. More recently, some of us discovered that (carbene)palladium(0)–diolefin complexes are extremely efficient catalysts for the reaction of 1,3-butadiene and methanol. With these complexes were obtained the best catalyst turnover numbers known so far for telomerizations (TON up to 300000).[11]

In this paper we describe a full account of our work on telomerization of 1,3-butadiene with alcohols in the presence of different palladium–carbene catalysts. Here, the synthesis and detailed characterization of four new (carbene)palladium(0)–diolefin complexes and a comparison with in situ generated catalysts in the palladium-catalyzed telomerization of 1,3-butadiene with methanol is presented. A significant improvement in catalyst productivity (TON $>$ 1500000) is observed by adding an excess of imidazolium salts to the reaction mixture. The optimized catalyst system is useful for telomerizations of a variety of aliphatic alcohols and substituted phenols.

Results and Discussion

As a starting point for our investigation, we synthesized different (carbene)palladium(0)–diolefin complexes (Figure 1). In order to mimic intermediates of the catalytic cycle we decided to use 1,3-dimethyldivinyl siloxane (dvds) as 1,6-diene ligand. Due to the increased acceptor strength of this diolefin compared with other 1,6-dienes[12] the corresponding palladium(0) complexes are stable for months and can be easily handled even under air.

First, the known complex (1,3-dimesitylimidazol-2-ylidene)-palladium(0)-η^2,η^2-1,1,3,3-tetramethyl-1,3-divinyl-disiloxane (**8**, [IMesPd(dvds)]) was synthesized by reacting the palladium(0) diallylether complex [$Pd_2(dae)_3$][13] with 1,3-dimesitylimidazol-2-ylidene carbene (IMes)[14] in 1,1,3,3-tetramethyl-1,3-divinyl-disiloxane (dvds) at −30°C. The new complexes (1,3-dimesityl-4,5-dimethylimidazol-2-ylidene)-palladium(0)-η^2,η^2-1,1,3,3-tetramethyl-1,3-divinyl-disiloxane (**9**), (1,3-dimesityl-4,5-dichloroimidazol-2-ylidene)-palladium(0)-η^2,η^2-1,1,3,3-tetramethyl-1,3-divinyl-disiloxane (**10**), and {1,3-bis-(2,6-diisopropylphenyl)imidazol-2-ylidine}-palladium(0)-η^2,η^2-1,1,3,3-tetramethyl-1,3-divinyl-disiloxane (**11**, [IPrPd(dvds)]), {1,3-bis-(2,6-diisopropylphenyl)-4,5-dimethyl-

imidazol-2-ylidine}-palladium(0)-η^2,η^2-1,1,3,3-tetramethyl-1,3-divinyl-disiloxane (**12**, [MeIPrPd(dvds)]) were obtained by reacting stoichiometric amounts of the corresponding free carbene with a Pd^0/dvds solution (8%) in THF and subsequent crystallization from *n*-pentane at −30 °C.

In order to rationalize catalytic effects as a function of structural features of the complexes we were interested in the detailed structural information of **8**–**12**. It is noteworthy that despite the catalytic potential of palladium(0)–carbene complexes[15] so far there exist only a small number of crystal structures of such complexes.[16] Nevertheless, suitable crystals for X-ray crystallography were obtained in all cases by crystallization from pentane or hexane at low temperature (< 0 °C). The crystallographic data of **8**–**12** are given in Table 1 and selected distances and angles are given in Table 2.

As shown in Figure 1 the central palladium atom is coordinated by the diolefin unit $H_2C{=}CHSiMe_2OSiMe_2HC{=}CH_2$ and the corresponding carbene ligand in a trigonal planar coordination in **8**–**12**. The plane (γ^1) of the carbene hetero-

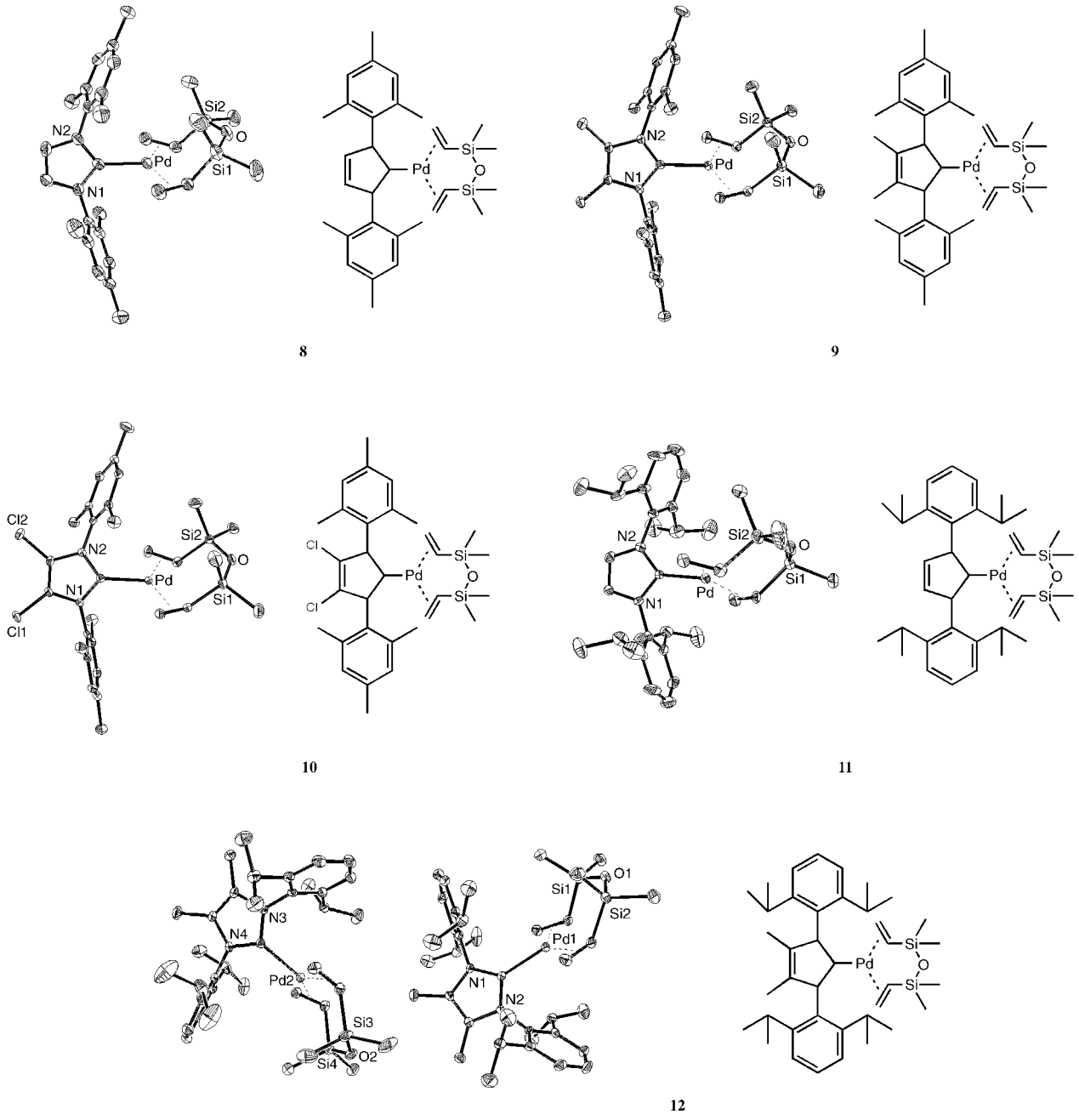

Figure 1. Monocarbenepalladium(0)–dvds complexes **8**–**12**. Hydrogen atoms are omitted for clarity; the thermal ellipsoids correspond to 30% probability.

Table 1. Crystallographic data.

	9	10	11	12
crystal system	monoclinic	monoclinic	orthorhombic	triclinic
space group	$P2_1/n$	$P2_1/n$	$P2_12_12_1$	$P\bar{1}$
a [Å]	12.865(3)	12.869(3)	12.893(3)	11.079(2)
b [Å]	17.157(3)	17.138(3)	13.899(3)	17.721(4)
c [Å]	15.903(3)	15.884(3)	20.645(4)	19.684(4)
α [°]				84.50(3)
β [°]	112.56(3)	112.79(3)		89.92(3)
γ [°]				84.96(3)
V [Å^3]	3241.6(11)	3229.7(11)	3699.6(14)	3831.8(14)
Z	4	4	4	4
ρ_{calcd} [g cm^{-3}]	1.281	1.370	1.223	1.230
$\mu(Mo_{K\alpha})$ [mm^{-1}]	0.671	0.838	0.593	0.576
T [K]	200	200	200	200
no. rflns (measd)	9596	7886	16781	11514
no. rflns (indep)	5198	4161	4833	11514
no. rflns (obsd)	4322	3533	4364	9274
no. params	335	358	370	823
$R1$ ($I>2\sigma(I)$)	0.039	0.033	0.027	0.033
$wR2$ (all data)	0.112	0.089	0.056	0.106

Table 2. Selected bond lengths [Å] and angles [°] in complexes **8**–**12**.

	8[11]	9	10	11	12
Pd–C(carbene)	2.076(5)	2.093(3)	2.080(3)	2.084(3)	2.114(3)/2.114(3)
Pd–CE[a]	2.028	2.048	2.054	2.032	2.056/2.059
	2.051	2.045	2.050	2.034	2.057/2.052
C=C(carbene)	1.320(6)	1.341(5)	1.330(5)	1.335(5)	1.352(4)/1.349(4)
C=C(olefin)	1.408(6)	1.409(5)	1.394(5)	1.409(6)	1.391(5)/1.395(5)
	1.388(6)	1.402(5)	1.398(6)	1.377(5)	1.398(5)/1.396(5)
C(carbene)–N	1.369(6)	1.365(4)	1.368(4)	1.370(4)	1.362(4)/1.362(4)
	1.373(5)	1.369(4)	1.376(4)	1.376(4)	1.369(3)/1.366(4)
N-C(carbene)-N	102.0(4)	102.7(3)	103.1(3)	102.2(3)	103.3(2)/103.1(2)
N-C(carbene)-Pd	128.7(4)	128.4(2)	127.9(2)	125.1(2)	125.0(2)/124.4(2)
	129.3(3)	128.9(2)	129.0(2)	131.9(2)	131.3(2)/132.0(2)
CE1-Pd-CE2	130.3	129.6	129.5	129.1	129.9/130.3
C(carbene)-Pd-CE	115.3	115.3	115.3	112.3	112.3/111.0
	114.3	114.9	115.0	118.2	117.1/118.0
γ^1[b]	64.7	59.2	58.8	73.8	56.5/57.9
γ^2[c]	76.6	77.4	77.2	82.3	69.7/70.6
γ^3[c]	77.7	81.3	80.6	88.7	72.0/76.2

[a] CE: mid-points of the coordinated C=C bonds. [b] γ^1 angle between the planes defined by the carbene heterocycle and the coordination plane. [c] γ^2, γ^3 angle between the planes defined by the carbene heterocycle and the aryl plane.

cycle and the coordination plane form angles of 56.5–73.8° (Table 2). The distance between the palladium and the carbene carbon atom varies in between 2.076(5) and 2.114(3) Å, which is in the expected range.[17] Surprisingly, the substituents on the carbene backbone in **9** and **10** do not influence significantly the carbene–palladium bond length. In **12** an elongation of the carbene–palladium bond length is observed.

For a detailed comparison of the complexes we have also carried out high level density functional theory calculations. In our modeling, the whole carbene ligand composition was used, while the diolefin ligand, 1,3-dimethyldivinyl siloxane ($H_2C{=}CHSiMe_2OSiMe_2HC{=}CH_2$) was replaced by two ethylene molecules. All complexes studied (**8′**–**12′**) have C_2 symmetry and are energy minimum structures on the potential energy surface according to the frequency calculations at the B3LYP/LANL2DZ level of theory (see computational part). The distances (Å) and angles (degree), and energies at the B3LYP/LANL2DZp level are used for comparison and discussion.

As given in Table 3, the computed bond lengths and angles are very close to X-ray data in Table 2. The computed Pd–$C_{carbene}$ and Pd–C_{Et} bond lengths are longer than the X-ray data by an average value of 0.052 and 0.046 Å, respectively. The difference for the C=C and N–$C_{carbene}$ bond lengths within the five-membered ring is only 0.026 and 0.010 Å, respectively. The angle differences are less than 1°. However, large differences are found for the torsion angle between the two planes in **9′** (7.6°), **10′** (9.3°) and **11′** (−17.4°), while those in **8′** and **12′** are much smaller (−1.6 and 1.2/0.2°), respectively.

Next, we tested palladium(0)–monocarbene complexes **8**–**12** in the telomerization of 1,3-butadiene with methanol. In addition, two (allyl)palladium(II)–(carbene) complexes **13** {[(IMes)Pd(allyl)Cl], IMes = 1,3-bis(2,4,6-trimethylphenyl)-imidazol-2-ylidene} and **14**[18] {[(IPr)Pd(allyl)Cl], IPr = 1,3-bis(2,6-diisopropylphenyl)imidazol-2-ylidene} and several in situ catalyst systems, for example, $Pd(OAc)_2/PPh_3$ were examined for comparison. To be of interest for practical application and to distinguish catalyst productivity a comparably small amount of catalyst (1,3-butadiene/catalyst 100000:1) was used in all experiments.

As shown in Table 4 (entries 1–4, 6, 7) the presence of N,N-diarylcarbene ligands is crucial for obtaining good yields and selectivity as well as high catalyst productivity. Using standard reaction conditions (70 °C, methanol/butadiene 2:1, 1 mol % NaOMe) the palladium(0)–monocarbene complexes **8** and **10** give nearly quantitative yield (96 %) of the desired telomers **1** and **2**, excellent chemoselectivity (> 99 %) and an *n*/*iso* ratio of 98:2 (Table 4, entries 1 and 3), while the "classic" phosphine catalyst system ($Pd(OAc)_2$/3 equiv PPh_3) gives only a product yield of 26 % and a significant lower chemoselectivity (Table 4, entry 8). Interestingly, 1,3-bis-(2,6-diisopropylphenyl)imidazol-2-ylidine palladium complexes **11** and **14** are less efficient and less selective compared with the 1,3-dimesitylimidazol-2-ylidine palladium complexes **8** and **13** (Table 4, entries 4, 7 vs 1, 6). Methyl substitution in the backbone of the carbene in com-

Table 3. Computed bond lengths [Å] and angles [°] for complexes **8′**–**12′**.

	8′	**9′**	**10′**	**11′**	**12′**
Pd–C(carbene)	2.1334	2.1396	2.1278	2.1415	2.1625
Pd–CE[a]	2.0910	2.0908	2.0971	2.0901	2.0950
C=C(carbene)	1.3622	1.3674	1.3629	1.3609	1.3663
C=C(olefin)	1.4032	1.4031	1.4016	1.4022	1.4006
C(carbene)–N	1.3766	1.3736	1.3789	1.3797	1.3788
N-C(carbene)-N	102.79	102.79	103.69	102.59	102.73
N-C(carbene)-Pd	128.60	128.61	128.16	128.71	128.64
CE1-Pd-CE2	124.62	123.96	123.70	124.70	122.05
C(carbene)-Pd-CE	117.69	118.02	118.02	117.65	118.97
γ^{1}[b]	63.05	66.81	68.05	56.36	57.66
γ^{2}[c]	100.11	96.50	96.56	104.37	105.77
γ^{3}[c]	81.50	85.10	84.51	78.54	75.22

[a] CE: mid-points of the coordinated C=C bonds. [b] γ^{1} angle between the planes defined by the carbene heterocycle and the coordination plane. [c] At the B3LYP/LANL2DZp level. γ^{2} and γ^{3} are the two torsion angles of the phenyl ring to the carbene center.

plex **12** decreased dramatically the catalyst performance. Apparently, substitution in the backbone of the mesitylsubstituted–carbene ligand (position 4 and 5) and the co-ligands (allyl or 1,6-diene) have only a minor influence on the yield and selectivities after 16 h. Unfortunately, all N,N-dialkyl-substituted imidazol-2-ylidine ligands showed basically no catalyst activity under our conditions (Table 4, entries 10–12). An in situ generated system from $Pd(OAc)_2$ and IMesHCl forms apparently the same catalytic species as complex **8** and also leads to good catalyst performance (Table 4, entries 1, 9).

While all experiments shown in Table 4 were run for 16 h, we also performed catalyst activity studies in which conversion and product yield were continuously measured. In Figures 2 and 3 selected runs are shown at different temperatures (general conditions: 0.001 mol% Pd, 15 g 1,3-butadiene, 25 mL THF, 5 mL isooctane as internal standard, 1 mol% NaOMe, 1,3-butadiene/MeOH 1:2). Using complex **8** at 90 °C, the reaction is very fast and nearly complete after only 2–3 h. At 70 °C the reaction requires approximately 6 h to reach completion, while at 50 °C 80% conversion is obtained after 16 h.

The study of activity of complexes **8**–**11** at 70 °C demonstrates the influence of different substitutions on the 4,5-position at the mesitylcarbene backbone (Figure 3). The dichlorosubstituted dimesitylcarbene complex **10** is faster than the unsubstituted complex **8**, while the dimethyl-substituted dimesitylcarbene complex **9** is slower than **8**. Diisopropylphenyl substitution in complex **11** instead of mesityl substitution in complex **8** leads to a significantly lower reaction rate and product yield.

In order to gain more insight into the relative stability and reactivity of these complexes upon carbene ligand coordination, we considered the ligand exchange reaction of complex **8′** shown in Scheme 3 as a model system. For a given complex, a positive reaction enthalpy (endothermic) indicates its reduced relative stability, while a negative reaction enthalpy (ΔH, exothermic) reveals the enhanced relative stability with regard to **8′**.

On the basis of these calculations, that the introduction of two methyl groups at the five-membered ring stabilizes complex (**9′**) by 2.1 kcal mol^{-1}, and this indicates that complex (**9′**) should be more stable (less active) in the catalytic reac-

Table 4. Telomerization of 1,3-butadiene with methanol in the presence of different catalysts.[a]

Entry	Catalyst	Yield [%][b]	*n*:*iso* [%]	Chemosel. [%][c]	TON (**1+2**)[d]	TOF (**1+2**)[d]
1	**8**	96	98:2	>99	96000	6000
2	**9**	93	98:2	99	93000	5813
3	**10**	96	98:2	>99	96000	6000
4	**11**	90	92:8	97	90000	5625
5	**12**	2	91:9	–	2000	125
6	**13**	94	98:2	99	94000	5875
7	**14**	46	92:8	96	46000	2875
8	$Pd(OAc)_2$/3 equiv PPh_3	26	96:4	87	26000	1625
9	$Pd(OAc)_2$/4 equiv IMesHCl	94	98:2	> 99	94000	5875
10	$Pd(OAc)_2$/4 equiv 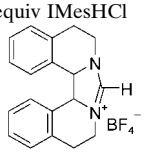	5	98:2	71	7000	438
11	$Pd(OAc)_2$/4 equiv 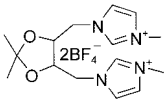	0	–	–	–	–
12	$Pd(OAc)_2$/4 equiv[e] 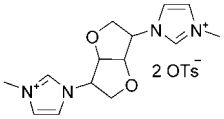	0	–	–	–	–

[a] General conditions: 16 h, 70 °C, 1 mol% NaOMe, MeOH/1,3-butadiene 2:1. [b] Yield of **1+2**. [c] Chemoselectivity = (**1+2**)/(**1+2+6+**VCH) × 100; VCH = 4-vinylcyclohexene. [d] Calculated with respect to 1,3-butadiene. [e] Ligand was prepared by Dr. A. Dervisi, synthetic details will be provided elsewhere.

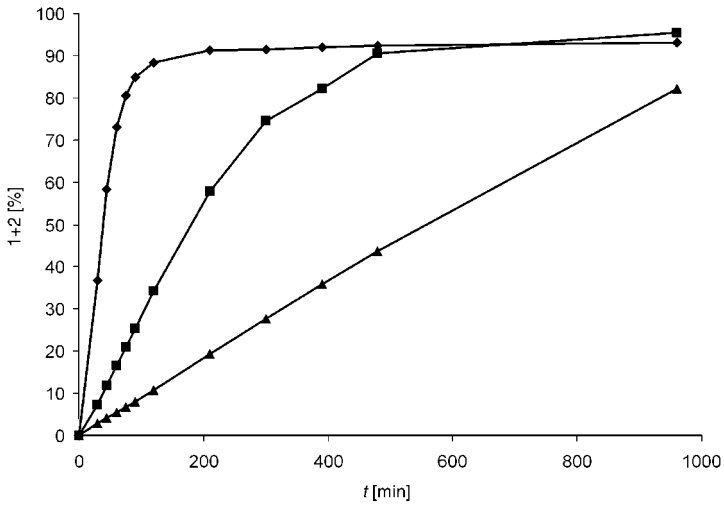

Figure 2. Catalyst performance of complex **8** at 50, 70 and 90 °C; ◆: 90 °C, ■: 70 °C, ▲: 50 °C.

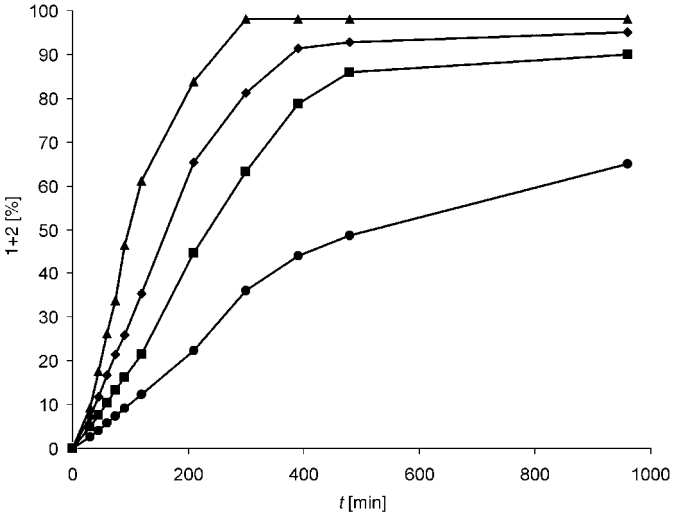

Figure 3. Activity of complexes **8**–**11** at 70 °C; ◆: complex **8**; ■: complex **9**; ▲: complex **10**; ●: complex **11**.

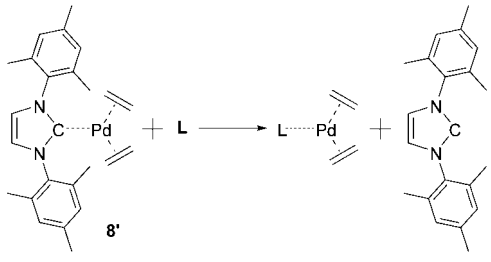

Scheme 3. Modeling of the carbene ligand exchange reaction of **8′**; ΔH (**9′**) = −2.1 kcal mol^{-1}, ΔH (**10′**) = +1.6 kcal mol^{-1}, ΔH (**11′**) = +2.4 kcal mol^{-1}, ΔH (**12′**) = +6.5 kcal mol^{-1}.

tion. In contrast, two chlorine substitutions at the backbone destabilize complex (**10′**) by 1.6 kcal mol^{-1}, and this reveals that complex (**10′**) should display enhanced destabilization and activity. These results are in agreement with the observed reactivity profiles shown in Figure 3.

Both the stabilizing effect in **9′** and the destabilizing effect in **10′** are electronic in origin; that is, an electron donating methyl group stabilizes the different palladium–carbene complexes and most likely reduces the reactivity of the intermediate **4** (see catalytic cycle, Scheme 2), while an electron withdrawing chlorine substitution destabilizes the palladium–carbene complexes and promotes the reactivity of **4** in the rate determining reaction step. Apart from the electronic effect, we were also interested in the contribution of the steric effect to catalyst stability. Instead of a mesityl group at the nitrogen centers, we used 2,6-diisopropylphenyl with the hope that the four isopropyl groups can influence coordination of substrates. Apparently, the calculated positive reaction enthalpy of 2.4 kcal mol^{-1} indicates the destabilization of complex **11′**. An even stronger destabilizing effect (+6.5 kcal mol^{-1}) is found for complex **12′**, despite of the electron donating substitution of methyl group at the backbone. Structural analysis reveals that the origin of destabilization in **12′** is due to the repulsive interaction between the methyl groups of the five-membered ring and the isopropyl group (the shortest H···H distance in **12′** is 2.086 Å, while it is 2.742 Å in the free carbene ligand, respectively). The consequence is the rotation of the benzene rings (γ^2 and γ^3) and the longer Pd–C(carbene) distance (Table 3), which reduces the catalyst activity.

However, this enhanced reactivity does not lead to the corresponding activity, as found in Figure 3. For example, the reaction with catalyst **11** is much slower and the corresponding yield is lower, as compared to catalyst **8**. The total yield with catalyst **12** is only 2% (Table 4, entry 5), and we did not consider it further. Therefore, the steric effect of the bulky isopropyl substituents at the benzene rings destabilize the catalyst on one hand, and on the other hand reduces its catalytic reactivity.

Economic calculations clearly show that the productivity shown above is still not sufficient in order to allow industrial bulk chemical applications using 1,3-butadiene. Here, catalyst turnover numbers in the range of 1 000 000 have to be realized at high product yield. Therefore, we were interested in further optimizing this catalyst system. Selected results from more than 300 experiments are shown in Table 5.

Most experiments were performed in the presence of catalysts **8** and **13** with a 1,3-butadiene to Pd ratio of 1 000 000:1 at 90 °C. At this temperature the reaction is somewhat faster, but both catalysts exhibit comparable stability. With or without ligand in the absence of palladium no product formation is observed at low conversion (< 5% formation of vinylcyclohexene, which results from the Diels–Alder reaction of 1,3-butadiene) (Table 5, entry 1). Simply using catalysts **8** and **13** under the conditions described in Table 4 telomers **1** and **2** are obtained in low yield (ca. 20%), which corresponds to a turnover number of 200 000 (Table 5, entries 2 and 3). Again both catalysts do not differ significantly in their productivity. Among various co-ligands, the addition of imidazolium salts proved to be beneficial for the reaction. By gradually increasing the amount of IMes·HCl as a precursor for the carbene ligand, the yield of the desired telomers increased to 91% (TON = 910 000) (Table 5, entries 4–9). By adding IMes·HCl in the presence

Table 5. Optimization of catalyst productivity for the telomerization of 1,3-butadiene with methanol.[a]

Entry	Cat.	Catalyst [mol %][a]	Ligand [mol %]	Yield [%][b]	*n*:*iso* [%]	Chemosel. [%][c]	TON (**1+2**)[d]	TOF[d]
1	–	0	0.004	0	–	0	0	0
2	**8**	0.0001	–	20	98:2	89	200000	12500
3	**13**	0.0001	–	19	98:2	90	190000	11875
4	**8**	0.0001	0.0002	17	98:2	88	170000	10625
5	**8**	0.0001	0.0004	40	98:2	95	400000	25000
6	**8**	0.0001	0.001	69	98:2	97	690000	43125
7	**8**	0.0001	0.002	87	98:2	98	870000	54375
8	**8**	0.0001	0.004	91	98:2	99	910000	56875
9	**13**	0.0001	0.004	89	98:2	98	890000	55625
10	**8**	0.00005	0.004	77	98:2	99	1540000	96250

[a] General conditions: 16 h, 90 °C, 1.0 mol % NaOMe, MeOH/1,3-butadiene 2:1, L = IMesHCl. [b] Yield of **1+2**. [c] Chemoselectivity = (**1+2**)/(**1+2+6+**VCH) × 100; VCH = 4-vinylcyclohexene. [d] Calculated with respect to 1,3-butadiene.

of only 0.5 ppm of **8** a good product yield (77 %) is observed (Table 5, entry 10). This corresponds to the *highest* catalyst productivity (TON = 1540000) and activity (TOF = 96250 h^{-1} after 16 h) reported for *any telomerization reaction*. Interestingly, the observed regioselectivity does not change with respect to the ligand concentration. This result is contradictory to our findings with palladium/phosphine catalysts.[7] Apparently during the catalytic cycle there is always only one carbene ligand bound to the central metal atom (reaction path A in Scheme 2).

Having demonstrated the excellent performance of **8** and **13** in the telomerization reaction of methanol, we were interested in the coupling of 1,3-butadiene with other alcohols. Again our molecular defined carbene complexes proved to be excellent catalysts.[11] Other alcohols, which were tested applying the standard conditions as described above, include *n*-butanol, *n*-hexanol isopropanol, benzyl alcohol, 2-methoxyethanol, 2-methylphenol, and 2,6-dimethylphenol. The results are summarized in Table 6. The activities and chemoselectivities for the linear telomers are also excellent using higher aliphatic alcohols in the presence of the mesityl-substituted complexes **8** and **9** (Table 6, entries 2 and 3, 8 and 9, 12–17). In addition to aliphatic alcohols, the telomerization of phenols proceeds reasonably well in the presence of palladium–carbene catalysts. Interestingly, the more-substituted phenol gave the best yield (86 %) in this reaction, which might be attributed to the higher basicity of 2,4,6-trimethylphenol compared to *o*-cresol (Table 6, entries 18–20).

Conclusion

In conclusion, we have synthesized monocarbene–palladium(0) complexes, which constitute excellent catalysts for the telomerization of 1,3-butadiene with various alcohols. Four new palladium(0)–carbene complexes have been characterized by X-ray crystallography, which allows for a systematic comparison of structure and catalyst performance. Density functional theory calculations of different palladium–carbene complexes show that the electron donating substitution of methyl group at the carbene backbone stabilizes the catalyst and reduces the reactivity of the corresponding intermediate (most likely **4**) in the rate determining step, while electron withdrawing substitution of chlorine destabilizes the catalyst and promote the reactivity.

By carefully optimizing the telomerization reaction of methanol unprecedented catalyst productivity (TON > 1500000) and activity (TOF = 100000 h^{-1}) are observed in the presence of an excess of imidazolium salt. For the first time bulk telomerization reactions appear to be commercially viable and are not limited by catalyst costs. The industrial applicability of our catalyst system has been already demonstrated by the production of telomers on a ton scale. In addition to methanol other aliphatic alcohols and substituted phenols react highly selectively in good to excellent yields, to produce the corresponding telomers. The reactions described in this study constitute prime examples of green chemistry.

Experimental Section

General procedure for telomerization reaction: [IMesPd^{0}dvds] (**8**; 1.6 mg, 2.77×10^{-6} mol) was dissolved in methanol (17.8 g, 0.555 mol). Subsequently NaOMe (149.5 mg, 2.77×10^{-3} mol) was added. The mixture was transferred under argon into a secured 100 mL stainless steel Parr autoclave. The autoclave was cooled with dry ice and 1,3-butadiene (15.0 g, 2.77×10^{-1} mol) was condensed in a separate 75 mL pressure cylinder (mass control). The given amount of 1,3-butadiene was condensed into the cooled autoclave and the vessel was heated to the desired reaction temperature. After 16 h the autoclave was cooled to room temperature and the remaining 1,3-butadiene was condensed. Isooctane (5 mL) as internal standard was added. The yield of telomerization products was determined by GC using an HP 6869A gas chromatograph. In order to isolate the different octadienyl ethers the reaction mixture was distilled in vacuo.

***cis/trans* 1-Methoxyocta-2,7-diene (1)**: b.p. (5 Torr) 35 °C; ^{1}H NMR ($CDCl_3$, 300 MHz): δ = 1.49 (q, J = 8.0 Hz, 2H), 2.68–2.76 (m, 4H), 3.31 (s, 3H), 3.86 (dd, J = 6, 2 Hz, 2H), 4.95–4.99 (m, 2H), 5.49–5.61 (m, 1H), 5.64–5.87 (m, 2H); ^{13}C NMR ($CDCl_3$, 75 MHz): δ = 26.97, 28.30, 28.73, 31.69, 33.21, 57.67, 57.90, 68.13, 73.25, 114.58, 126.30, 126.47, 133.29, 134.44, 138.54, 138.62.

3-Methoxyocta-2,7-diene (2): b.p. (5 Torr) 35 °C; ^{1}H NMR ($CDCl_3$, 300 MHz): δ = 1.34–1.68 (m, 4H), 2.01–2.10 (m, 2H), 3.26 (s, 3H), 3.46–3.54 (m, 1H), 4.90–5.20 (m, 2H), 5.14–5.22 (m, 1H), 5.58–5.87 (m, 2H); ^{13}C NMR ($CDCl_3$, 75 MHz): δ = 24.62, 33.70, 34.81, 56.14, 82.92, 114.53, 117.03, 138.72, 138.85.

8-Butoxyocta-1,6-diene: b.p. (5 Torr) 80 °C; ^{1}H NMR ($CDCl_3$, 400 MHz): δ = 5.7–5.5 (m, 2H), 5.45–5.36 (m, 1H), 4.9–4.7 (m, 2H), 3.7 (dd, J = 6, 1 Hz, 2H), 3.26 (t, J = 6.7 Hz, 2H), 1.9 (m, 4H), 1.42 (quint, J = 7.1 Hz, 2H), 1.42 (quint, J = 7.1 Hz, 2H), 1.39 (q, $^3J_{5,4,6}$ = 7 Hz, 2H), 1.25 (sext, J = 7.1 Hz, 2H), 0.75 (t, J = 7.3 Hz, 3H); ^{13}C NMR ($CDCl_3$, 100 MHz): δ = 138.2, 133.5, 126.7, 114.3, 71.3, 69.1, 32.9, 31.6, 31.4, 28.05, 19.1, 13.6; MS: *m*/*z* (%): 182 (1.4) [M^+], 139 (4.3), 126 (10.6), 108 (24), 101 (3.9), 97 (11), 93 (27), 82 (35), 67 (72), 57 (100); HRMS: *m*/*z*: calcd for $C_{12}H_{22}O$: 182.16707, found: 182.16460.

Table 6. Telomerization of 1,3-butadiene with different alcohols.[a]

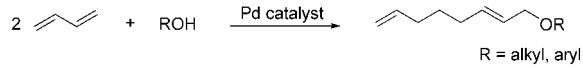

Entry	ROH	Cat.	Cat.[mol%]	Yield [%][b]	*n*:*iso*[%]	Chemosel. [%][c]	TON[d]	TOF
1	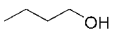	$Pd(OAc)_2$/3 equiv PPh_3	0.001	36	95:5	47	76000	4750
2	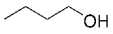	**8**	0.001	97	98:2	97	99500	6218
3	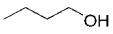	**9**	0.001	97	99:1	97	99500	6218
4	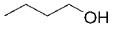	**10**	0.001	63	96:4	86	73000	4562
5	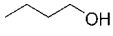	**11**	0.001	89	89:11	89	99500	6218
6	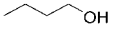	**12**	0.001	34	89:11	43	78000	4875
7		$Pd(OAc)_2$/3 equiv PPh_3	0.005	3	97:3	16	3800	238
8		**8**	0.005	82	98:2	82	20000	1250
9		**9**	0.005	85	99:1	85	20000	1250
10		**10**	0.005	68	98:2	68	20000	1250
11		**11**	0.005	37	99:1	37	19800	1238
12	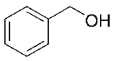	**8**	0.005	96	97:3	96	19200	1200
13	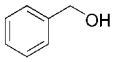	**9**	0.005	96	98:2	96	20000	1250
14	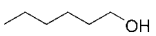	**8**	0.001	90	97:3	95	95000	5938
15	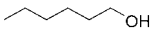	**9**	0.001	93	98:2	93	99800	6238
16	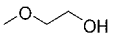	**8**	0.001	98	98:2	98	99800	6238
17	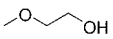	**9**	0.001	95	99:1	98	96500	6031
18		**8**	0.005	37	98:2	97	7600	475
19		**8**	0.005	56	84:16	97	11500	718
20	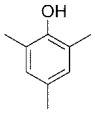	**8**	0.005	86	84:16	92	18600	1162

[a] General conditions: 16 h, 70 °C, 1.0 mol% NaOR, MeOH to 1,3-butadiene = 2 to 1. [b] Yield of telomers. [c] Chemoselectivity = (yield of telomers)/(yield of telomers+octatriene+VCH) × 100; VCH = 4-vinylcyclohexene. [d] Calculated with respect to 1,3-butadiene.

8-Hexyloxyocta-1,6-diene: b.p. 90 °C; ^{1}H NMR ($CDCl_3$, 400 MHz): δ = 5.8–5.4 (m, 3H), 5.1–4.9 (m, 2H), 3.9 (br d, J = 6.1 Hz, 2H), 3.3–3.4 (m, 2H), 2.1–2.0 (m, 4H), 1.9 (m, 4H), 1.6–1.4 (m, 4H), 1.4–1.2 (m, 6H), 0.9–0.8 (m, 3H); ^{13}C NMR ($CDCl_3$, 100 MHz): δ = 138.4, 133.7, 126.9, 114.4, 71.4, 70.1, 33.1, 31.6, 29.7, 28.2, 25.8, 22.5, 13.9; MS: *m*/*z* (%): 210 (0.6) [M^+], 126 (4.8), 109 (13), 97 (4), 93 (9), 82 (18), 67 (38), 57 (34), 43 (100); elemental analysis calcd (%) for $C_{14}H_{26}O$: C 79.94, H 12.46; found: C 79.88, H 12.76; HRMS: *m*/*z*: calcd for $C_{14}H_{26}O$: 210.19836, found: 210.19477.

8-Isopropoxyocta-1,6-diene: b.p. 50 °C; ^{1}H NMR ($CDCl_3$, 400 MHz): δ = 5.7–5.5 (m, 2H), 5.4–5.5 (m, 1H), 4.9–4.8 (m, 2H), 3.8 (dd, J = 5, 1 Hz, 2H), 3.5 (sept, J = 6.1 Hz, 1H), 2.0, 1.9 (m, 4H), 1.4 (quint, J = 7.5 Hz, 2H), 1.05 (d, J = 6.1 Hz, 6H); ^{13}C NMR ($CDCl_3$, 100 MHz): δ = 138.1, 132.8, 114.2, 70.2, 68.5, 32.9, 31.3, 27.9, 21.7, 127.7, 114., 133.7, 126.1,

114.1, 71.5, 68.5, 58.4, 58.3, 32.7, 31.1, 27.8; MS: *m/z* (%): 168 (0.11) [M^+], 126 (12.5), 109 (30.6), 97 (13), 93 (25), 82 (68), 67 (95), 55 (76), 43 (100); elemental analysis calcd (%) for $C_{11}H_{20}O$: C 78.51, H 11.98; found: C 78.56, H 11.95.

8-(2-Methoxyethoxy)octa-1,6-diene: ^{1}H NMR ($CDCl_3$, 400 MHz): $\delta =$ 5.7–5.5 (m, 2H), 5.4–5.5 (m, 1H), 4.9–4.7 (m, 2H), 3.8 (dd, $J = 5.4$, 1 Hz, 2H), 3.45–3.35 (m, 4H), 3.2 (s, 3H), 1.85–1.75 (m, 4H), 1.3 (quint, $J =$ 7.5 Hz, 2H); ^{13}C NMR ($CDCl_3$, 100 MHz): $\delta = 137.9$, 133.7, 126.1, 114.1, 71.5, 68.5, 58.4, 58.3, 32.7, 31.1, 27.8; MS: *m/z* (%): 183 (1.6) [M^+-1], 125 (4.7), 115 (9.1), 103 (6.3), 93 (23), 81 (23), 77 (29), 67 (100), 59 (47), 45 (23), 29 (17); HRMS: *m/z*: calcd for $C_{11}H_{20}O_2$: 184.14633, found: 184.14468.

Octa-2,7-dienyloxybenzene: ^{1}H NMR ($CDCl_3$, 400 MHz): $\delta = 7.6$–7.5 (m, 2H), 7.25–7.15 (m, 3H), 6.2–5.9 (m, 3H), 5.35–5.25 (m, 2H), 4.75 (dd, $J =$ 5, 1 Hz, 2H), 2.5–2.3 (m, 4H), 1.8 (quint, $J = 7.5$ Hz, 2H); ^{13}C NMR ($CDCl_3$, 100 MHz): $\delta = 158.5$, 138.3, 134.8, 129.2, 129.1, 125.1, 120.5, 114.5, 68.4, 33.1, 31.6, 27.9; MS: *m/z* (%): 202 (2.4) [M^+], 108 (9.9), 94 (100), 79 (10.9), 67 (55), 58 (11), 55 (24), 43 (40); HRMS: *m/z*: calcd for $C_{14}H_{18}O$: 202.13577, found: 202.13485.

1,3,5-Trimethyl-2-octa-2,7-dienyloxybenzene: ^{1}H NMR ($CDCl_3$, 400 MHz): $\delta = 6.9$ (s, 2H), 5.9–5.8 (m, 3H), 5.1–5.0 (m, 2H), 4.3 (d, $J =$ 5 Hz, 2 H), 2.35 (s, 6H), 2.3 (s, 3H), 2.2–2.1 (m, 4H), 1.6 (quint, $J =$ 7.5 Hz, 2H); ^{13}C NMR ($CDCl_3$, 100 MHz): $\delta = 153.7$, 138.5, 134.9, 132.8, 131.6, 129.2, 126.2, 114.5, 73.1, 33.1, 31.6, 28.1, 20.6, 16.3; MS: *m/z* (%): 244 (2.5) [M^+], 137 (56), 135 (50), 121 (74), 109 (11), 107 (11), 105 (14), 91 (83), 67 (39), 55 (35), 41 (100); HRMS: *m/z*: calcd for $C_{17}H_{24}O$: 244.18271 found: 244.18105.

1-Methyl-2-octa-2,7-dienyloxybenzene: ^{1}H NMR ($CDCl_3$, 400 MHz): $\delta =$ 7.45–7.4 (m, 2H), 7.15 (t, $J = 7.3$ Hz, 1H), 7.1 (d, $J = 6.3$ Hz, 1H), 6.2–6.0 (m, 3H), 5.35–5.25 (m, 2H), 4.7 (dd, $J = 5.5$, 1.2 Hz, 2H), 2.55 (s, 3H), 2.35–2.25 (m, 4H), 1.8 (quint, $J = 7.5$ Hz, 2H); ^{13}C NMR ($CDCl_3$, 100 MHz): $\delta = 156.8$, 138.5, 134.1, 130.6, 126.8, 126.6, 125.6, 120.3, 114.6, 111.3, 68.6, 33.1, 31.7, 28.2, 16.3; MS: *m/z* (%): 216 (2.7) [M^+], 108 (100), 90 (21), 79 (45), 67 (31), 55 (14), 53 (23), 51 (23), 41 (17); HRMS: *m/z*: calcd for $C_{15}H_{20}O$: 216.15141, found: 216.15059.

1,3-Dimesitylimidazol-2-yliden-palladium(0)-η²,η²-1,1,3,3-tetramethyl-1,3-divinyldi-siloxane (8): ^{1}H NMR ([D$_8$]THF, 400 MHz): $\delta = 7.34$ (s, 2H), 6.9 (d, $J = 0.6$ Hz, 4H), 2.62 (dd, $J = 12.1$, 1.4 Hz, 2H), 2.37 (dd, $J = 15.3$, 1.4 Hz, 2H), 2.25 (s, 6H), 2.1 (dd, $J = 15.3$, 12.1 Hz, 2H), 2.14 (s, 12H), 0.0 (s, 6H), −0.7 (s, 6H); ^{13}C NMR ([D$_8$]THF, 100 MHz): $\delta = 199.3$, 138.8, 138.5, 136.0, 129.4, 123.8, 58.3, 57.2, 20.9, 18.3, 1.5, −1.5; MS (FAB): *m/z* (%): 714 (20) [Pd(IMes)$_2$]$^+$, 596 (25) [M^+], 412 (50), 305 (100), 187 (15); elemental analysis calcd (%) for $C_{29}H_{42}N_2OPdSi_2$: C 58.32, H 7.09, N 4.69; found: C 58.5, H 7.35, N 4.69.

1,3-Dimesityl-4,5-dimethylimidazol-2-ylidene-palladium(0) η²,η²-1,1,3,3-tetramethyl-1,3-divinyl-disiloxane (9): ^{1}H NMR ([D$_8$]THF, 400 MHz): $\delta =$ 6.9 (s, 4H), 2.6 (dd, $J = 12.3$, 1.4 Hz, 2H), 2.39 (dd, $J = 15.3$, 1.4 Hz, 2H), 2.25 (s, 6H), 2.1 (s, 12H), 2.05 (dd, $J = 15.3$, 12.3 Hz, 2H), 1.9 (s, 6H), 0.0 (s, 6H), −0.8 (s, 6H); ^{13}C NMR ([D$_8$]THF, 100 MHz): $\delta = 196.4$, 138.8, 136.9, 136.5, 129.7, 126.7, 58.6, 57.1, 21.1, 18.3, 9.2, 1.6, −1.4; MS: *m/z* (%): 666 (20) [M^+], 480 (25), 373 (15), 337 (50), 301 (20), 171 (100), 143 (30), 117 (80), 59 (25).

1,3-Dimesityl-4,5-dichloroimidazol-2-ylidene-palladium(0) η²,η²-1,1,3,3-tetramethyl-1,3-divinyl-disiloxane (10): ^{1}H NMR ([D$_8$]THF, 400 MHz): $\delta = 7.34$ (s, 4H), 2.7 (dd, $J = 12.3$, 1.6 Hz, 2H), 2.45 (dd, $J = 15.4$, 1.6 Hz, 2H), 2.2 (dd, $J = 15.4$, 12.3 Hz, 2H), 2.3 (s, 6H), 2.14 (s, 12H), 0.0 (s, 6H), −0.8 (s, 6H); ^{13}C NMR ([D$_8$]THF, 100 MHz): $\delta = 191.9$, 140.3, 136.7, 134.9, 129.9, 60.1, 59.7, 21.1, 18.2, 1.5, −1.4; MS: *m/z* (%): 666 (20) [M^+], 480 (25), 373 (15), 337 (50), 301 (20), 171 (100), 143 (30), 117 (80), 59 (25); elemental analysis calcd (%) for $C_{29}H_{40}Cl_2N_2OPdSi_2$: C 52.29, H 6.05, N 4.21; found: C 52.30, H 6.2, N 4.12.

1,3-Bis-(2,6-diisopropylphenyl)imidazol-2-ylidine-palladium(0) η²,η²-1,1,3,3-tetra-methyl-1,3-divinyl-disiloxane (11): ^{1}H NMR ([D$_8$]THF, 400 MHz): $\delta = 7.66$ (s, 2H), 7.55 (t, $J = 7.7$ Hz, 2H), 7.43 (d, $J = 7.7$ Hz, 4H), 3.23 (sept, $J = 6.7$ Hz, 4H), 2.66 (d, $J = 12.7$ Hz, 2H), 2.49 (d, $J =$ 15.3 Hz, 2H), 2.28 (dd, $J = 12.7$, 15.3 Hz, 2H), 1.45 (d, $J = 6.7$ Hz, 12H), 1.34 (d, $J = 6.9$ Hz, 12H), 0.18 (s, 6H), −0.8 (s, 6H); ^{13}C NMR ([D$_8$]THF, 100 MHz): $\delta = 200.8$, 146.7, 138.5, 130.0, 125.2, 124.3, 59.5, 58.2, 29.3, 26.0, 23.2, 1.8, −1.2; MS: *m/z* (%): 681 (10) [M^+], 494 (33), 387 (100), 186 (10); elemental analysis calcd (%) for $C_{35}H_{55}N_2OPdSi_2$: C 61.69, H 7.99, N 4.11; found: C 61.82, H 8.13, N 4.21.

1,3-Bis-(2,6-diisopropylphenyl)-4,5-dimethylimidazol-2-ylidine-palladium(0) η²,η²-1,1,3,3-tetramethyl-1,3-divinyl-disiloxane (12): ^{1}H NMR ([D$_8$]THF, 400 MHz): $\delta = 7.38$ (dd, $J = 8.1$, 8.5 Hz, 2H), 7.25 (d, $J = 8$ Hz, 4H), 3.0 (sept, $J = 7$ Hz, 4H), 2.3 (dd, $J = 11.9$, 2 Hz, 2H), 2.2 (dd, $J =$ 15.5, 2 Hz, 2H), 2.05 (dd, $J = 15.5$, 11.9 Hz, 2H), 2.0 (s, 6H), 1.22 (d, $J =$ 6.9 Hz, 12H), 1.15 (d, $J = 6.9$ Hz, 12H), −0.4 (brs, 12H); ^{13}C NMR ([D$_8$]THF, 100 MHz): $\delta = 197.9$, 147.1, 137.1, 129.9, 127.6, 124.7, 60.3, 59.2, 29.1, 24.9, 24.3, 10.9, 0.0; MS: *m/z* (%): 708 (2.9) [M^+], 522 (13), 415 (58), 401 (26), 385 (5), 255 (10), 171 (100), 159 (18), 143 (42), 117 (80), 103 (13), 73 (28), 59 (29)elemental analysis calcd (%) for $C_{37}H_{58}N_2OPdSi_2$: C 61.64, H 8.24, N 3.95; found: C 62.48, H 8.38, N 3.81.

X-ray crystallographic studies of the complexes: Data were collected with a STOE-IPDS diffractometer using graphite-monochromated $Mo_{K\alpha}$ radiation. The structures were solved by direct methods (SHELXS-86: G. M. Sheldrick, *Acta Crystallogr.* **1990**, *A46*, 467) and refined by full-matrix least-squares techniques against F^2 (SHELXL-93: G. M. Sheldrick, University of Göttingen (Germany), **1993**) All nonhydrogen atoms were refined anisotropically. XP (BRUKER AXS) was used for structure representations.

CCDC-231 917–231 920 (**9**–**12**) contain the supplementary crystallographic data for this paper. These data can be obtained free of charge via www.ccdc.cam.ac.uk/conts/retrieving.html (or from the Cambridge Crystallographic Data Centre, 12 Union Road, Cambridge CB2 1EZ, UK; fax: (+44) 1223-336-033; or deposit@ccdc.cam.uk).

Computation: All calculations were carried out by using the Gaussian 98 program.[19] All structures were first optimized at B3LYP density functional level of theory with the LANL2DZ[20] basis set, and the nature of the optimized structures on the potential energy surface was characterized by the calculated number of imaginary frequency (NImag) at the same level of theory (B3LYP/LANL2DZ), i.e., minimum structures without (NImag = 0), and transition states with only one imaginary frequency (NImag = 1),[21] The related frequency calculations provided at the same time zero-point energies (ZPE) The obtained structures at B3LYP/LANL2DZ were further refined at the B3LYP level of theory with the LANL2DZ basis set including a set of polarization functions (B3LYP/LANL2DZp[20c]). The structures and energies at the B3LYP/LANL2DZp level were used for discussion. In the calculation, the real sized imidazolium ions were used, while the diolefin ligand was modeled by two ethylene molecules.

Acknowledgement

This work was supported by Degussa AG (Oxeno Olefinchemie GmbH) and the state of Mecklenburg-Vorpommern. Analytical services were provided by Mrs. S. Buchholz and Dr. C. Fischer (both IfOK). For catalyst development of the complexes **13** and **14** performed at the University of New Orleans, the National Science Foundation and the Louisiana Board of Regents are gratefully acknowledged.

[1] For reviews on telomerization reactions see: a) N. Yoshimura in *Applied Homogeneous Catalysis with Organometallic Compounds*, *Vol. 1* (Eds.: B. Cornils, W. A. Herrmann), VCH, Weinheim, **2000**, p. 361; b) J. Tsuji, *Palladium Reagents and Catalysts: Innovations in Organic Synthesis, Wiley, Chichester*, **995**, p. 422; c) J. M. Takacs in *Comprehensive Organometallic Chemistry II*, *Vol. 12* (Eds.: E. W. Abel, F. G. A. Stone, G. Wilkinson), Pergamon Press, Oxford, **1995**, p. 785; d) R. F. Heck, *Palladium Reagents in Organic Syntheses, Academic Press, London*, **985**; e) A. Behr, in *Aspects of Homogeneous Catalysis*, *Vol. 5* (Ed.: R. Ugo), Reidel, Dordrecht, **1984**, p. 3; f) W. Keim, A. Behr, M. Röper, in *Comprehensive Organometallic Chemistry*, *Vol. 8* (Eds.: G. Wilkinson, F. G. A. Stone, E. W. Abel), Pergamon Press, Oxford, **1982**, p. 372.

[2] Recent examples of telomerization reactions: a) A. Behr, M. Urschey, *Adv. Synth. Catal.* **2003**, *345*, 1242–1246; b) M. S. Viciu, F. K. Zinn, E. D. Stevens, S. P. Nolan, *Organometallics* **2003**, *22*, 3175–

3177; c) A. Behr, M. Urschey, *J. Mol. Catal.* **2003**, *197*, 101–113; d) U. Donze, C. Pinel, P. Gallezot, P. L. Taylor, *Adv. Synth. Catal.* **2002**, *344*, 906–910; e) G. S. Fonseca, R. F. de Souza, J. Dupont, *Catal. Commun.* **2002**, *3*, 377–380; f) V. Desvergnes-Breuil, C. Pinel, P. Gallezot, *Green Chem.* **2001**, *3*, 175–177.

[3] The current industrial price for 1,3-butadiene is in the range of 0.4–0.6 Euro kg^{-1}.

[4] N. Yoshimura, M. Tamura (Kuraray Company, Ltd.), US 4356333, **1981** [*Chem. Abstr.* **1982**, *96*, 103630s].

[5] a) B. Estrine, R. Soler, C. Damez, S. Bouquillon, F. Henin, J. Muzart, *Green Chem.* **2003**, *5*, 686–689; b) L. Magna, Y. Chauvin, G. P. Niccolai, J. M. Basset, *Organometallics* **2003**, *22*, 4418–4425; c) E. Drent, M. R. Eberhard, R. H. Van der Made, P. G. Pringle, **2003**, WO 2003040065; d) F. Vollmüller, W. Mägerlein, S. Klein, J. Krause, M. Beller, *Adv. Synth. Catal.* **2001**, *343*, 29–33; e) F. Benvenuti, C. Carlini, M. Marchionna, R. Patrini, A. M. Raspolli Galletti, G. Sbrana, *J. Mol. Catal.* **1999**, *140*, 139–155; f) M. Basato, L. Crociani, F. Benvenuti, A. M. Raspolli Galletti, G. Sbrana, *J. Mol. Catal.* **1999**, *145*, 313–316; g) R. Patrini, M. Lami, M. Marchionna, F. Benvenuti, A. M. Raspolli Galletti, G. Sbrana, *J. Mol. Catal.* **1998**, *129*, 179–189; h) P. Grenouillet, D. Neibecker, J. Poirier, I. Tkatchenko, *Angew. Chem.* **1982**, *94*, 796–797; *Angew. Chem. Int. Ed. Engl.* **1982**, *21*, 767–768; i) M. Perree-Fauvet, Y. Chauvin, *Tetrahedron Lett.* **1975**, 4559–4562; j) D. Commereuc, Y. Chauvin, *Bull. Soc. Chim. Fr.* **1974**, 652–656; k) J. Beger, C. Duschek, H. Füllbier, W. Gaube, *J. Prakt. Chem.* **1974**, *316*, 26–42; l) J. Beger, H. Reichel, *J. Prakt. Chem.* **1973**, *315*, 1067–1076; m) S. Takahashi, T. Shibano, N. Hagihara, *Tetrahedron Lett.* **1967**, 2451–2453.

[6] a) R. Benn, P. W. Jolly, T. Joswig, R. Mynott, K.-P. Schick, *Z. Naturforschung* **1986**, *41b*, 680–691; b) P. W. Jolly, R. Mynott, B. Raspel, K.-P. Schick, *Organometallics* **1986**, *5*, 473–481; c) P. W. Jolly, *Angew. Chem.* **1985**, *97*, 279–291; *Angew. Chem. Int. Ed. Engl.* **1985**, *24*, 283–295; for an alternative mechanistic proposal see: d) A. Behr, G. v. Ilsemann, W. Keim, C. Krüger, Y.-H. Tsay, *Organometallics* **1986**, *5*, 514–518; e) R. Benn, P. W. Jolly, R. Mynott, B. Raspel, G. Schenker, K.-P. Schick, G. Schroth, *Organometallics* **1985**, *4*, 1945–1953; f) A. Döhring, P. W. Jolly, R. Mynott, K.-P. Schick, G. Wilke, *Z. Naturforschung* **1981**, *36b*, 1198–1199.

[7] F. Vollmüller, S. Klein, J. Krause, W. Mägerlein, M. Beller, *Eur. J. Inorg. Chem.* **2000**, 1825–1832.

[8] a) B. Åkermark, S. Hansson, B. Krakenberger, A. Vitagliano, K. Zetterberg, *Organometallics* **1984**, *3*, 679–682; b) B. Åkermark, A. Vitagliano, *Organometallics* **1985**, *4*, 1275–1283; c) B. Åkermark, K. Zetterberg, S. Hansson, B. Krakenberger, A. Vitagliano, *J. Organomet. Chem.* **1987**, *335*, 133–142.

[9] The current price is US$ 8.50 per gram Pd (Financial Times; 14.01.2004).

[10] M. Gómez Andreu, A. Zapf, M. Beller, *Chem. Commun.* **2000**, 2475–2476.

[11] a) R. Jackstell, M. Gomez Andreu, A. C. Frisch, H. Klein, K. Selvakumar, A. Zapf, A. Spannenberg, D. Röttger, O. Briel, R. Karch, M. Beller, *Angew. Chem.* **2002**, *114*, 1028–1031; *Angew. Chem. Int. Ed.* **2002**, *41*, 986–989; b) R. Jackstell, A. C. Frisch, M. Beller, D. Röttger, M. Malaun, B. Bildstein, *J. Mol. Catal.* **2002**, *185*, 105–112.

[12] J. Krause, K.-J. Haack, G. Cestaric, R. Goddard, K.-R. Pörschke, *Chem. Commun.* **1998**, 1291–1292.

[13] J. Krause, G. Cestanic, K.-J. Haack, K. Seevogel, W. Storm, K.-R. Pörschke, *J. Am. Chem. Soc.* **1999**, *121*, 9807–9823.

[14] A. J. Arduengo, H. V. R. Dias, R. L. Harlow, M. Kline, *J. Am. Chem. Soc.* **1992**, *114*, 5530–5534.

[15] Recent examples from 2001 on: a) A. C. Frisch, N. Shaik, A. Zapf, M. Beller, *J. Mol. Catal.* **2004**, in press; b) A. C. Frisch, F. Rataboul, A. Zapf, M. Beller, *J. Organomet. Chem.* **2003**, *687*, 403–409; c) K. Selvakumar, A. Zapf, M. Beller, *Org. Lett.* **2002**, *4*, 3031–3033; d) A. M. Magill, D. S. McGuinness, K. J. Cavell, G. J. P. Britovsek, V. C. Gibson, A. J. P. White, D. J. Williams, A. H. White, B. W. Skelton, *J. Organomet. Chem.* **2001**, *617*, 546–560; e) A. Fürstner, A. Leitner, *Synlett* **2001**, 290–292; f) W. A. Herrmann, V. P. W. Böhm, C. W. K. Gstöttmayr, M. Grosche, C.-P. Reisinger, T. Weskamp, *J. Organomet. Chem.* **2001**, *617–618*, 616–628; g) D. S. McGuinness, N. Saendig, B. F. Yates, K. J. Cavell, *J. Am. Chem. Soc.* **2001**, *123*, 4029–4040; h) D. J. Nielsen, K. J. Cavell, B. W. Skelton, A. H. White, *Organometallics* **2001**, *20*, 995–1000; i) C. L. Yang, H. M. Lee, S. P. Nolan, *Org. Lett.* **2001**, *3*, 1511–1514; j) L. Jafarpour, S. P. Nolan, *Adv. Organomet. Chem.* **2001**, *46*, 181–222; k) C. J. Mathews, P. J. Smith, T. Welton, A. J. P. White, D. J. Williams, *Organometallics* **2001**, *20*, 3848–3850; l) E. Peris, J. A. Loch, J. Mata, R. H. Crabtree, *Chem. Commun.* **2001**, 201–202.

[16] a) K. Selvakumar, A. Zapf, A. Spannenberg, M. Beller, *Chem. Eur. J.* **2002**, *8*, 3901–3906; b) L. R. Titcomb, S. Caddick, F. G. N. Cloke, D. J. Wilson, D. McKerrecher, *Chem. Commun.* **2001**, 1388–1389; c) C. W. K. Gstöttmayr, V. P. W. Böhm, E. Herdtweck, M. Grosche, W. A. Herrmann, *Angew. Chem.* **2002**, *114*, 1421–1422; *Angew. Chem. Int. Ed.* **2002**, *41*, 1363–1365; d) R. Weiss, N. Kraut, *Angew. Chem.* **2002**, *114*, 327–329; *Angew. Chem. Int. Ed.* **2002**, *41*, 311–314.

[17] a) L. Xu, W. Chen, J. F. Bickley, A. Steiner, J. Xiao, *J. Organomet. Chem.* **2000**, *598*, 409–416, and references therein; b) T. Weskamp, F. J. Kohl, W. Hieringer, D. Gleich, W. A. Herrmann *Angew. Chem.* **1999**, 111, 2573–2576; *Angew. Chem. Int. Ed.* **1999**, *38*, 2416–2419; b) W. A. Herrmann, M. Elison, J. Fischer, C. Köcher, G. R. J. Artus, *Angew. Chem.* **1995**, *107*, 2602–2605; *Angew. Chem. Int. Ed. Engl.* **1995**, *34*, 2371–2374; c) C. K. Lee, J. C. C. Chen, K. M. Lee, C. M. Liu, I. J. Lin, *Chem. Mater.* **1999**, *11*, 1237–1242; d) B. Bildstein, M. Malaun, H. Kopacka, K.-H. Ongania, K. Wurst, *J. Organomet. Chem.* **1998**, *552*, 45–61; e) W. A. Herrmann, L. J. Gooßen, M. Spiegler, *J. Organomet. Chem.* **1997**, *547*, 357–366.

[18] a) S. S. Cammerer, M. S. Viciu, E. D. Stevens, S. P. Nolan, *Synlett* **2003**, 1871–1873; b) N. Marion, O. Navarro, R. A. Kelly, S. P. Nolan, *Synthesis* **2003**, 2590–2592; c) M. S. Viciu, F. K. Zinn, E. D. Stevens, S. P. Nolan, *Organometallics* **2003**, *22*, 3175–3177; d) M. S. Viciu, O. Navarro, R. F. Germaneau, R. A. Kelly III, W. Sommer, N. Marion, E. D. Stevens, L. Cavallo, S. P. Nolan, *Organometallics* **2004**, *23*, 1629–1635.

[19] Gaussian 98 (Revision A.7), M. J. Frisch, G. W. Trucks, H. B. Schlegel, G. E. Scuseria, M. A. Robb, J. R. Cheeseman, V. G. Zakrzewski, J. A. Montgomery, Jr., R. E. Stratmann, J. C. Burant, S. Dapprich, J. M. Millam, A. D. Daniels, K. N. Kudin, M. C. Strain, O. Farkas, J. Tomasi, V. Barone, M. Cossi, R. Cammi, B. Mennucci, C. Pomelli, C. Adamo, S. Clifford, J. Ochterski, G. A. Petersson, P. Y. Ayala, Q. Cui, K. Morokuma, D. K. Malick, A. D. Rabuck, K. Raghavachari, J. B. Foresman, J. Cioslowski, J. V. Ortiz, B. B. Stefanov, G. Liu, A. Liashenko, P. Piskorz, I. Komaromi, R. Gomperts, R. L. Martin, D. J. Fox, T. Keith, M. A. Al-Laham, C. Y. Peng, A. Nanayakkara, C. Gonzalez, M. Challacombe, P. M. W. Gill, B. G. Johnson, W. Chen, M. W. Wong, J. L. Andres, M. Head-Gordon, E. S. Replogle, J. A. Pople, Gaussian, Inc., Pittsburgh, PA, **1998**.

[20] a) P. J. Hay, W. R. Wadt, *J. Chem. Phys.* **1985**, *82*, 299–310; b) T. H. Dunning Jr. , P. J. Hay, *Modern Theoretical Chemistry* (Ed.: H. F. Schaefer III), Plenum, New York, **1976**, p. 1; c) for polarization functions see: S. Huzinaga, J. Anzelm, M. Klobukowski, E. Radzio-Andzelm, Y. Sakai, H. Tatewaki, *Gaussian Basis Sets for Molecular Calculations*, Elsevier, Amsterdam, **1984**.

[21] J. B. Foresman, Æ. Frisch, *Exploring Chemistry with Electronic Structure Methods: A Guide to Using Gaussian*, 2nd ed., Gaussian, Inc., Pittsburgh PA, **1996**.

Received: February 23, 2004
Published online: June 21, 2004

